CONF-950793--10
BNL-62136

State-Resolved Dynamics of Infrared Photodesorption of CO from Ag(111)

L. Fleck, B. Niu, R. J. Beuhler and Michael G. White

Chemistry Department, Brookhaven National Laboratory, Upton, NY 11973

1. INTRODUCTION

Current understanding of the dynamics of photon stimulated desorption (PSD) of molecules from surfaces has been derived in large part from state- and energy-resolved probes of the desorbed molecules in the gas-phase.[1,2] Analogous to studies of gas-phase photodissociation, information concerning the electronic interactions and nuclear motions on the dissociative potential surface are inferred from the energy, internal state and angular distributions of the photoproducts. Of particular interest is the use of state-resolved methods to ellucidate the photodesorption mechanism which can involve substrate and/or absorbate excitations followed by facile energy transfer between the electronic and nuclear degrees of freedom. The primary concern of this work is desorption induced by photon energies well below the work function ($\leq 1-2$ eV) which is nominally assumed to occur via a thermally activated process. From a dynamical standpoint, laser-induced surface heating results from the rapid thermalization of initially photoexcited electron-hole pairs which relax through inelastic $e^- - e^-$ scattering and energy transfer to lattice modes of the substrate. Desorption results from random surface atom displacements which deposit vibrational energy in the absorbate-metal bond in excess of the binding energy. The desorption rate is highest at the maximum surface temperature (T_{max}) induced by the laser pulse which can be determined with reasonable accuracy from a classical heat-diffusion model.[3-5] As a result, "thermally" desorbed molecules are expected to have internal and translational energy distributions characteristic of T_{max}.

State-resolved measurements performed by Buntin, *et al.*[6] for NO/Pt(111) at a number of photon energies between 0.65 eV and 3.49 eV have identified two desorption channels, with the "slow" velocity component exhibiting near Boltzmann rotational and translational distributions. Although the measured angular distribution, photon energy dependence and translational energies of the slow channel are consistent with thermally activated desorption, the translational energies did not show a dependence on laser fluence as expected from the classical heat-diffusion model, *i.e.* $T_{max} \propto I_0$. In addition, the rotational temperature (~ 100 K) was found to be significantly smaller than the expected surface temperature rise ($T_{max} = 227$ K). In a related study, Prybyla, *et al.* observed a Boltzmann rotational state distribution for NO desorbed from Pd(111) at 2.33 eV (532 nm), however, the derived rotational temperature was approximately half that of the surface temperature.[7] Such "rotational cooling" has been attributed to strong coupling between rotation and translation induced by the molecule-surface potential and its anisotropy with respect to molecular orientation.[7,8]

In this work, we present state-resolved measurements for IR (1.17 eV, 1064 nm) photodesorption of CO physisorbed on a Ag(111) surface. In contrast to NO, there has been very little

experimental work on CO photodesorption, partly due to the difficulties associated with multiphoton or VUV probes required to obtain state-resolved dynamics. Recent state-resolved measurements for CO/Pt(111),[9] CO/NiO(111)/Ni(111)[10] and CO/Cr_2O_3/Cr(110)[11] have focussed on the observation of non-Boltzmann final state distributions induced by UV excimer radiation (308 nm, 248 nm and 193 nm) at laser fluences too low to induce substantial thermal desorption. The low desorption temperatures for both the monolayer (48 K) and multilayer (36 K) phases of CO/Ag(111), however, permit the study of photo-induced "thermal" processes at modest laser power densities. Furthermore, the low surface temperature and weak interaction between the CO molecule and the Ag(111) surface favors equilibration of the rovibronic and translational energies with T_{max}. State-resolved detection of desorbed CO is performed via $(1+1')$ resonant multiphoton ionization (REMPI) using coherent VUV radiation and time-of-flight mass spectrometry. The observed rotational and translational state distributions are well described by Maxwell-Boltzmann distributions with characteristic temperatures which indicate near equilibration of the rotational and translational degrees of freedom. These results are consistent with a photo-induced "thermal" desorption mechanism and are compared with the predictions of the classical heat-diffusion model.

2. EXPERIMENTAL

A schematic diagram of the experimental apparatus and associated lasers is shown in Fig. 1. The main features of the apparatus are a windowless VUV generation chamber and doubly-differentially pumped capillary light guide, an open-cycle liquid helium (LHe) cooled sample manipulator and a differentially-pumped time-of-flight (TOF) mass spectrometer.

Coherent VUV radiation in the range 115.2 - 114.9 nm needed to probe the desorbed CO molecules via $(1+1')$ REMPI is generated by $2\omega_{uv}+\omega_{vis}$ non-resonant, sum frequency mixing in Xe gas near the $5p \rightarrow 7s$ atomic resonance.[12] Collinear visible (576.0–574.5 nm; ~40 mj/pulse; 0.07 cm^{-1}, 20 Hz) and UV (288.0–287.3 nm; ~5 mj/pulse) laser beams were focussed by a 100 mm focal length achromatic lens (Optics for Research) inside the small beam chamber and into a pulsed, free jet expansion of Xe. The latter is produced by a piezo-driven, pulsed molecular beam valve fitted with a 1 mm nozzle and using a 1300 Torr stagnation pressure. Typical beam densities close to the nozzle are 5-10 Torr with a background pressure of $\sim 10^{-2}$ Torr as maintained by a 270 l/sec turbomolecular pump. The diverging fundamentals (visible and UV) and sum frequency VUV radiation are captured by a pyrex capillary tube (35 cm long; 1 mm id.) and directed into the surface chamber where it passes between two parallel grids which define the extraction field for the TOF spectrometer. The capillary has two small, isolated breaks within a differential pumping section, the first being pumped by a mechanical pump and the second by a small (50 l/sec) turbomolecular pump. A differential pressure of $\sim 10^8$ is maintained by the capillary light guide. The coherent VUV radiation is detected for optimization and normalization procedures by a photodiode constructed of Pt foil mounted inside the surface chamber. The VUV intensity at the spectrometer is estimated to be $\sim 10^9 - 10^{10}$ photons per pulse, with an energy bandwidth of 0.7 cm^{-1}. Further details concerning the VUV source and photodiode can be found in Ref.s [13,14].

The Ag(111) crystal is mounted at the bottom of a rotatable, LHe cooled cryostat (Janis ST-400) via a combination of Pt and Ta support wires. The Pt post (0.8 mm) provides thermal

DISCLAIMER

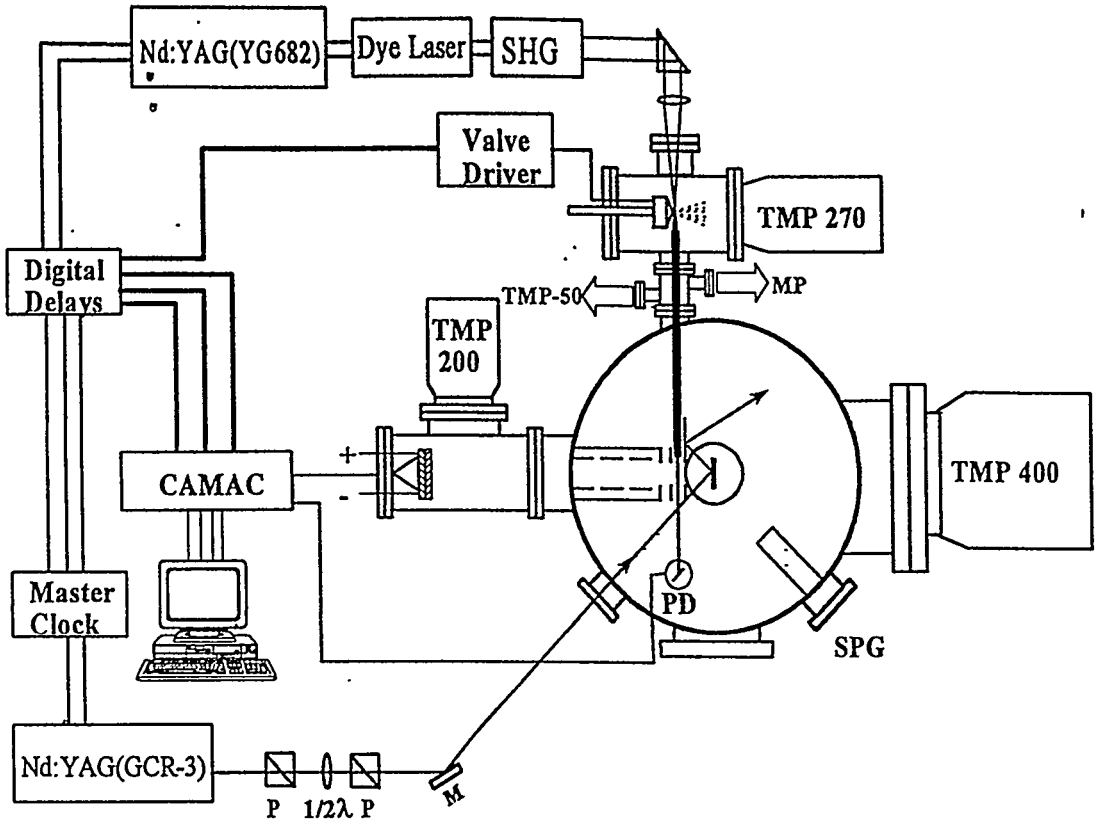

Figure 1: Schematic diagram of experimental apparatus.

contact to the bottom of the LHe dewar while the Ta wire connections (0.64 mm) are used for resistive heating required for annealing. The temperature of the crystal was monitored by a type E thermocouple (nickel-chromium alloy) spot-welded to the Pt wire in contact with the crystal. For multilayer and monolayer studies, the crystal temperature was held at 30 K and 42 K, respectively, with a heater located at the bottom of the LHe dewar and an automatic temperature controller (Lake Shore 312). The electropolished, oriented Ag(111) single crystal was obtained commercially (Monocrystals) and cleaned in UHV by repeated Ar ion sputtering and annealing ($\sim$ 730 K) cycles.

For the measurements presented here, the 1064 nm fundamental of a pulsed Nd:YAG laser (Quanta-Ray GCR3, 20 Hz) was used as the desorption source. A Glan-Thompson prism polarizer (Lambrecht) and $1/2\lambda$ plate are used to establish p-polarized light relative to the crystal surface and a second polarizer is used for setting the incident IR power. The collimated IR beam was apertured to a 0.5 cm (dia.) spot incident on the crystal at 45°. Neutral molecules desorbed along the surface normal were probed by VUV radiation in the extraction region of the TOF mass spectrometer. Reflected IR radiation from the crystal is directed away from the interaction region of the spectrometer by a small gold mirror mounted on the back of the first ion extraction electrode. For the data presented in this work, the IR laser fluence incident on the Ag(111) crystal was $\sim$ 45 mj/cm^2. Given that the reflectivity of Ag at 45° is 98%,[15] the actual fluence absorbed by the crystal is 0.9 mj/cm^2. The distance from the crystal to the VUV laser beam is 2.5 cm which defines the neutral flight path for velocity measurements. The TOF mass

spectrometer incorporates Wiley-McLaren spatial focussing with an extraction field of 52 V/cm and a total flight path of 45 cm. Ions are detected by a 40 mm (dia.) dual channel plate array and TOF mass spectra are obtained by a CAMAC controlled, 200 MHz transient digitizer (LeCroy 8828D) triggered by the VUV probe laser. Rotational spectra are obtained by scanning the VUV laser frequency while monitoring the TOF spectrum gated on the CO^+ mass peak. Time-of-flight arrival distributions are collected by scanning the delay between the desorption and VUV probe lasers via a CAMAC controlled delay generator (LeCroy 2323A). The latter are used to derive velocity and translational energy distributions of the desorbing molecules as discussed below.

Desorbed CO molecules are detected by $(1 + 1')$ REMPI via the rovibrationally-resolved $B\ ^1\Sigma^+\ (v,\ J) \leftarrow X\ ^1\Sigma^+\ (v'',\ J'')$ transition. Coherent VUV radiation is used to photoexcite ground state molecules to specific rovibrational levels of the B state which are subsequently ionized by the unseparated UV radiation (288.0–287.3 nm). Due to the high intensity of the unconverted UV radiation, the VUV excitation step is rate limiting. Consequently, the ion intensities are given by the one-photon $B-X$ line strengths and the rovibronic state populations of the desorbed molecules. Rottke and Zacharias have shown that (VUV+UV) REMPI spectra via the $B-X$ transition is suitable for extracting rotational state populations for $v''=0$ as well as having very high detection sensitivity ($\sim 4 \times 10^5$ per cm^3 per quantum state).[16]

3. RESULTS AND DISCUSSION

3.1 CO Binding on Ag(111)

In a previous study using high resolution energy loss spectroscopy (HREELS), thermal desorption spectroscopy (TDS) and angle resolved photoemission (ARPES), Hansen, *et al.* have shown that CO forms a stable, physisorbed monolayer on Ag(111) with a desorption temperature of $\sim$ 50 K.[17] The observation of the CO stretch vibration (265 meV) in HREELS spectrum indicated that at least some of the physisorbed CO molecules have orientations perpendicular (or nearly so) to the surface. The latter are required for the observation of the dipole-excited energy loss peak which would otherwise be absent for CO molecules lying parallel to the surface. An earlier ARPES study of monolayer CO on Ag(111), however, concluded that the photoemission data is consistent with a parallel, in-plane orientation.[18] Hansen, *et al.* conclude that all the available data suggests that CO in the monolayer phase is randomly oriented, unlike physisorbed CO and N_2 on graphite which have in-plane orientations with a $(2\sqrt{3} \times \sqrt{3})$ "herringbone" structure as determined by LEED measurements.[19] At lower surface temperatures ($\leq$ 40 K) and higher exposures, a multilayer phase becomes evident which is assumed to be ordered like bulk CO and incommensurate with the Ag(111) surface structure.[17]

In Figure 2 we show TDS curves for CO desorption following a 10L exposure of the Ag(111) crystal held at 22 K. Although these desorption curves are for CO molecules desorbed in the $v''=0,\ J''=0$ quantum state, we do not expect the desorption temperatures to exhibit a final state dependence as they primarily reflect the CO binding energies and desorption kinetics. The upper panel of Fig. 1 shows two peaks corresponding to desorption of the multilayer and monolayer phases at 36 K and 47 K, respectively. These desorption temperatures are in good agreement with the previous measurements of Hansen *et al.*[17] but the desorption peaks are much

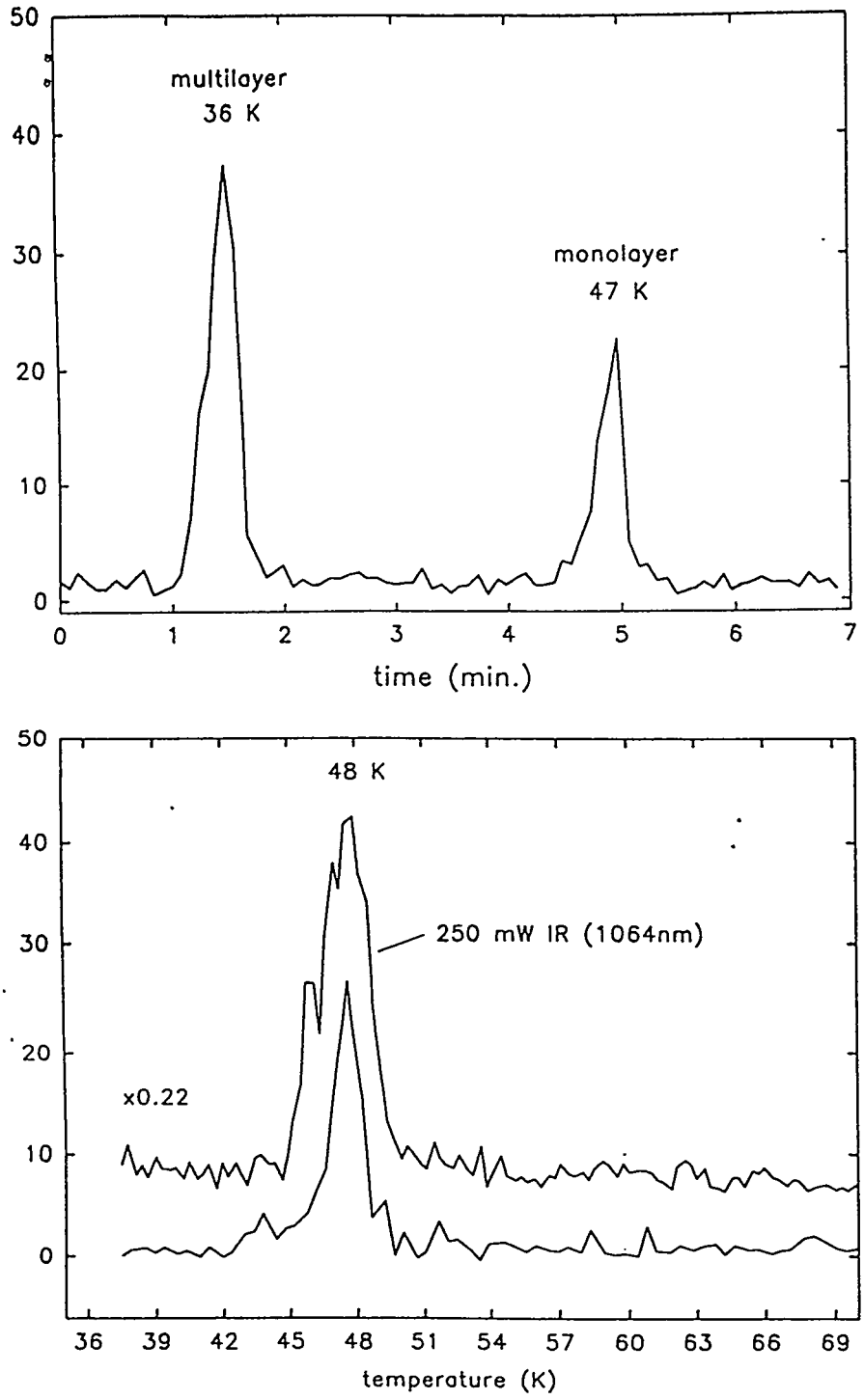

Figure 2: Thermal desorption spectra for CO physisorbed on Ag(111). Upper panel: Thermal desorption of CO multilayer and monolayer phases with the Ag(111) crystal initially at 22 K. Lower panel: Comparison of thermal desorption of CO monolayer with and without IR (1064 nm) irradiation. The Ag(111) crystal was initially at 42 K.

sharper (~ 1 K FWHM). The monolayer and multilayer phases are well separated in temperature, allowing laser-induced desorption studies to be performed on the monolayer by dosing the crystal at temperatures near 40 K. This is shown in the lower panel of Figure 2 along with a TDS curve taken with the crystal exposed to the IR beam (250 mW). The initial crystal temperature was held at 38 K and only monolayer desorption is observed. With simultaneous IR irradiation, the detected TDS yield for the monolayer is greatly enhanced, a factor of ~ 5 in Fig. 2, and the desorption peak width is also increased. Signal enhancements as high as 10 – 20 times were also observed depending on the incident IR fluence. As all the CO molecules are removed from the surface in both TDS measurements, the observed incease with IR irradiation must come from an incease in the flux of desorbed molecules into the detection solid angle defined by the VUV laser beam. This suggests that IR radiation causes a narrowing of the desorption angular distribution along the surface normal or an increase in the production of the final rovibronic state relative to thermal desorption ($v'' = 0$, $J'' = 0$ in Fig. 2). It is generally assumed, however, that laser-induced thermal processes will exhibit angular distributions which are comparable to direct surface heating, *i.e.* $\cos\theta$. The increase in width of the TDS-IR peak is most likely a result of IR laser "pre-heating" of the substrate which lowers the activation energy for desorption.

3.2 Desorption Cross Section

Exposure of monolayer coverages of CO on Ag(111) to the IR laser results in rapid depletion of the surface molecules within the exposed area of the surface. The latter can be measured by setting the VUV probe laser to a specific rovibronic transition and following the signal decay as a function of IR exposure. Such a depletion curve is shown in Figure 3 for photodesorbed CO molecules in the $J'' = 5$ rotational level. The depletion curves are well fit by a bi-exponential describing the rapid decay at short times (0-10 min) and the nearly flat tail at long times. Bi-exponential depletion curves have also been observed for CO desorption from NiO(111)/Ni(111) surfaces at photon energies of 4.0 eV[10] and 3.82 eV.[20] Considerable variation in the fast decay component is observed for other CO rotational states but the slow decay component is essentially idependent of J''. The observed depletion rates can be used to obtain desorption cross sections through the expression

$$ln(I/I_0) = -n\sigma t$$

where n is the surface coverage (molecules/cm^2) and σ (cm^2) is the desorption cross section.[21] For the depletion curves observed in this work, we obtain IR-desorption cross sections of $(5 - 20) \times 10^{-16}$ cm^2 (fast decay) and 8×10^{-17} cm^2 (slow decay) assuming a monolayer coverage of 5×10^{14} molecules/cm^2. These values are significantly larger than those measured for UV photodesorption of CO from Pt(111) (3.5×10^{-19} cm^2),[9] Cr_2O_3 (3.5×10^{-17} cm^2)[11] and NiO(111) (3.3×10^{-18} cm^2 and 4.5×10^{-19} cm^2).[10] The large cross sections measured here may reflect the small transient surface temperature rise (~ 10 K) that is required break the weak CO-Ag(111) physisorption bond (0.27 eV, Ref. [22]).

Depletion curves such as that shown in Fig. 3 are also required for intensity corrections of arrival time and rotational spectra, discussed below, which require data accumulation times on the order of 20-30 min.

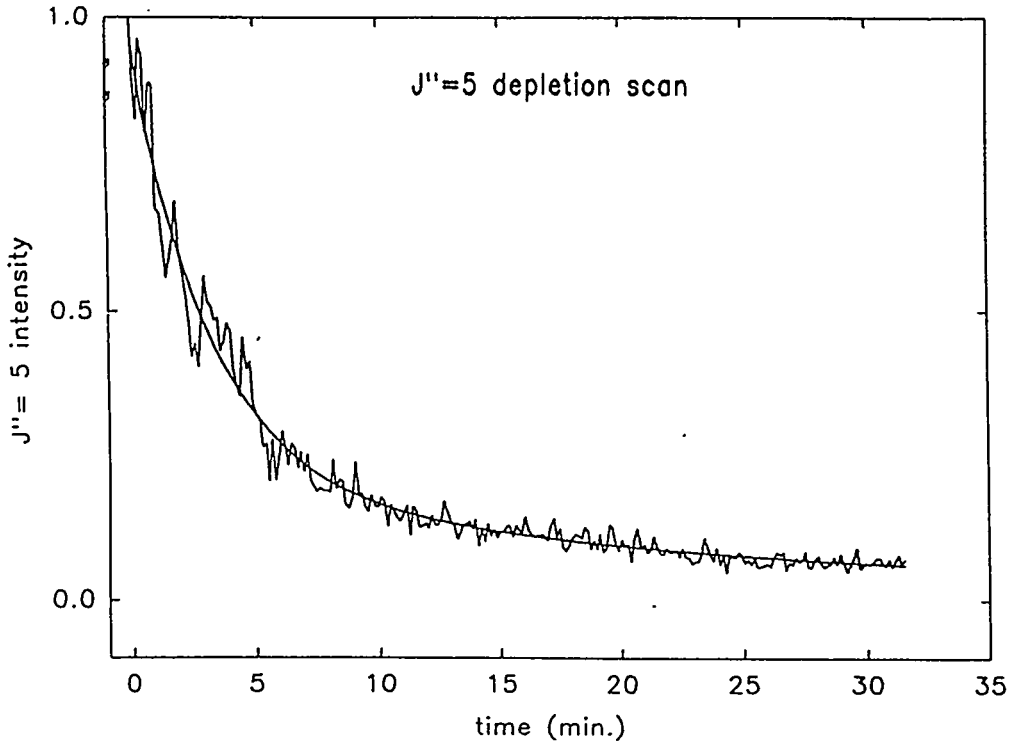

Figure 3: IR-induced depletion curve for desorbed CO molecules in the $J'' = 5$ rotational state.

3.3 Translational Distributions

Information on the velocity distributions of desorbed CO molecules is derived from arrival time spectra obtained by scanning the delay between the IR-desorption laser and the VUV probe laser. The surface normal is oriented along the axis of the mass spectrometer so that these measurements probe primarily the component of the velocity distribution perpendicular to the surface plane ($v_\perp$). The arrival time spectrum for CO molecules desorbed from the monolayer in $J'' = 5$ and from the multilayer in $J'' = 1$ are shown in Figure 4. The data were corrected for the time-dependent depletion of the CO molecules (see Fig. 3). Also shown are calculated arrival time distributions assuming Boltzmann velocity distributions with a characteristic translational temperature. The calculations utilize the flux weighted velocity distribution, $v^3\ exp[-mv^2/2kT]$ and include corrections for the arrival time spread resulting from the finite collection solid angle. For the latter we assumed that the CO molecules desorb with a $\cos\theta$ angular distribution relative to the surface normal as expected for thermal desorption.[1] The calculated curves are in very good agreement with the observed arrival time distributions (Fig. 4) indicating that $v_\perp$ can be described by a thermal distribution. Arrival time spectra for other rotational levels up to $J'' = 8$ are also well fit by simple Boltzmann velocity distributions with similar translational temperatures. For monolayer coverages and an IR fluence of 45 mj/cm^2, the translational temperature averaged over all the measured rotational states is 110 ± 10 K. Arrival time measurements for CO molecules desorbed from multilayer coverages result in a somewhat lower translational temperature, 90 ± 10, which must reflect, in part, the lower surface temperature for the multilayer (30 K) versus the monolayer experiments (42 K).

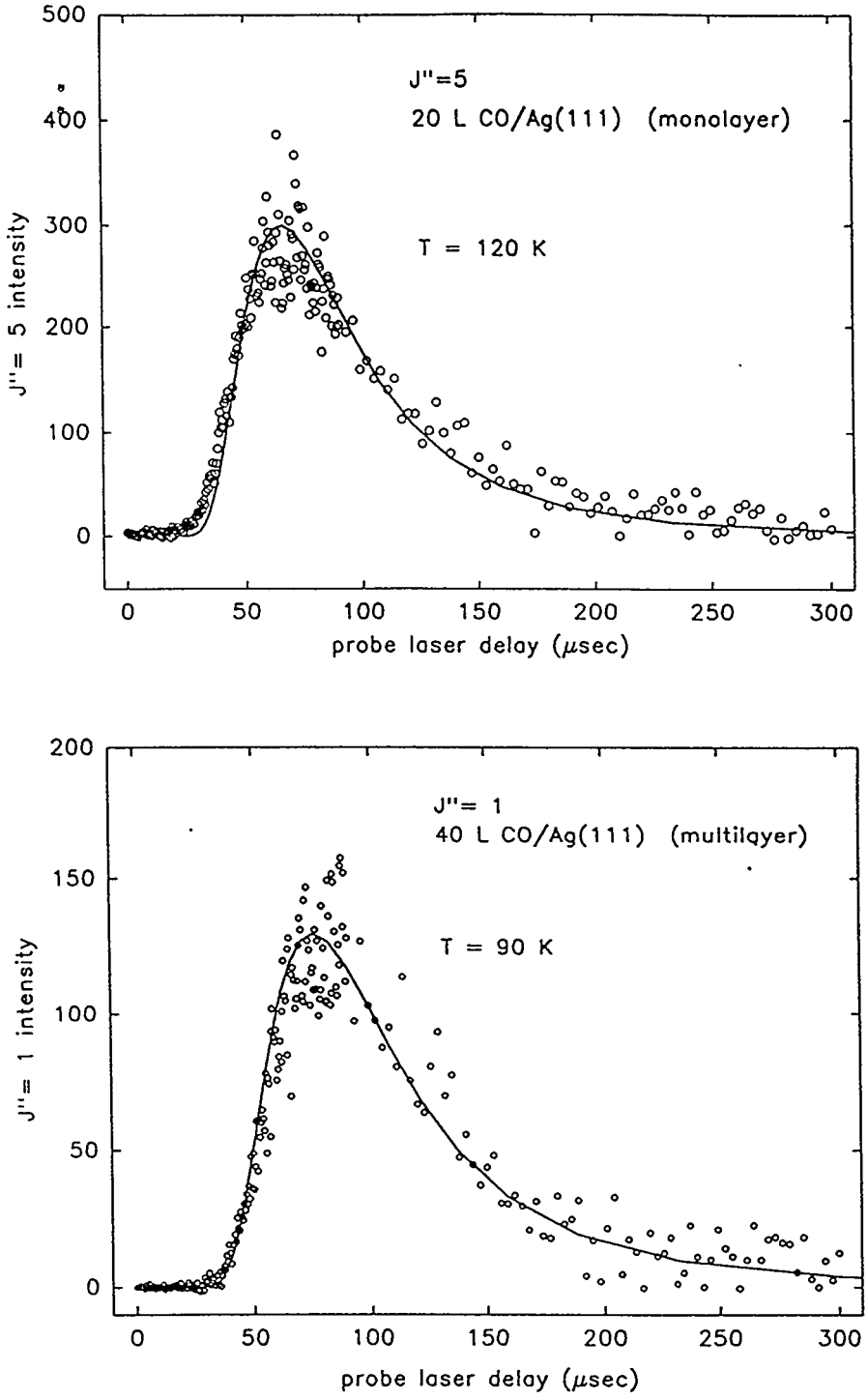

Figure 4: Arrival time distributions for state-selected CO molecules photodesorbed from Ag(111) at 1064 nm. The solid lines represent calculated arrival time distributions based on Boltzmann velocity distributions. Upper panel: CO monolayer (42 K), $J'' = 5$, calculated translational temperature of 120 K. Lower panel: CO multilayer (30 K), $J'' = 1$, calculated translational temperature of 90 K.

3.4 Rotational Distributions

The R-branch $(J'' + 1 \leftarrow J'')$ portion of the $B,\ v = 0 \leftarrow X,\ v'' = 0$ REMPI spectrum for CO molecules desorbed with $v_\perp = 350$ m/sec is shown in the upper panel of Figure 5. This velocity corresponds to the observed peak in the arrival distributions of CO at monolayer coverages (see Fig. 4). Ground state rotational distributions are derived from the observed line intensities by dividing by the one-photon rotational line strength, which is simply given by $S_{J''+1} = J'' + 1$.[23] A thermal (Maxwell-Boltzmann) rotational population distribution is proportional to $exp[-BJ''(J''+1)/kT]$ and a semilog plot of rotational state populations versus $J''(J''+1)$ results in a straight line from which the rotational temperature can be derived. A Boltzmann plot of the rotational populations derived from the REMPI spectrum is shown in the lower panel of Figure 5. The derived rotational populations are reasonably well described by a thermal distribution with a characteristic rotational temperature of 108 K and a value of 103 ± 7 K is obtained averaging over several measurements. This rotational temperature is quite close to the derived translational temperature of 110 ± 10 K, indicating essentially complete equilibration of the translational and rotational degrees of freedom. This result is consistent with a thermally activated desorption process, yet such equilibration of rotational and translational energies has not been previously observed in other low energy, laser-induced desorption studies.[1,2,7] In particular, "rotational cooling" is not observed, suggesting that the CO-Ag(111) interaction potential does not have a strong orientational dependence which results in weak coupling between "frustrated" rotation and translational motions. This conclusion is consistent with the nearly random orientation of CO on Ag(111) at low coverage as suggested by Hansen, *et al.*[17] In this regard, IR-induced desorption measurements on N_2, and NO would be of interest since molecular beam scattering measurements indicate that the orientational anisotropy of the M-Ag(111) interaction potential is less for N_2 and comparable for NO.[24]

Rotational spectra obtained at $v_\perp = 500$ m/sec yielded slightly higher rotational temperatures, 120 ± 10 K, which results in a positive correlation between translational and rotational energies. Again, this result is consistent with a thermal desorption mechanism in which the rotational and translational energies are equilibrated with the surface temperature at the instant of desorption.

3.5 Comparison with Classical Heat-Diffusion Model

As noted in the Introduction, laser-induced surface heating can be described by a classical heat-diffusion model which provides a reasonable estimate for the temperature "jump" associated with pulsed laser excitation.[3-5] The maximum transient temperature rise is given by

$$\Delta T_{max} = \left(\frac{8}{3K}\right)\left(\frac{\kappa}{\pi}\right)^{1/2}(1-R)I_0\left(\frac{t_0}{4-t_r/t_0}\right)^{1/2}$$

where K and κ are the thermal conductivity and diffusivity, respectively, R is the reflectivity and I_0 is the incident power density. This expression assumes a triangular pulse shape characterized by a rise time, t_r, and a pulse width of t_0. For Ag at 40 K, the thermodynamic quantities are $K = 1.1 \times 10^3$ j/m-sec-K and $\kappa = 1.2 \times 10^{-3}$ m^2/sec.[25] From spatial distribution measurements of the IR beam cross section, we estimate the power density to be $(4.2 - 7.7) \times 10^6$ W/cm^2. The IR pulse can be characterized by $t_r \sim t_0 = 1 \times 10^{-8}$ sec and the reflectivity of Ag for p-polarized

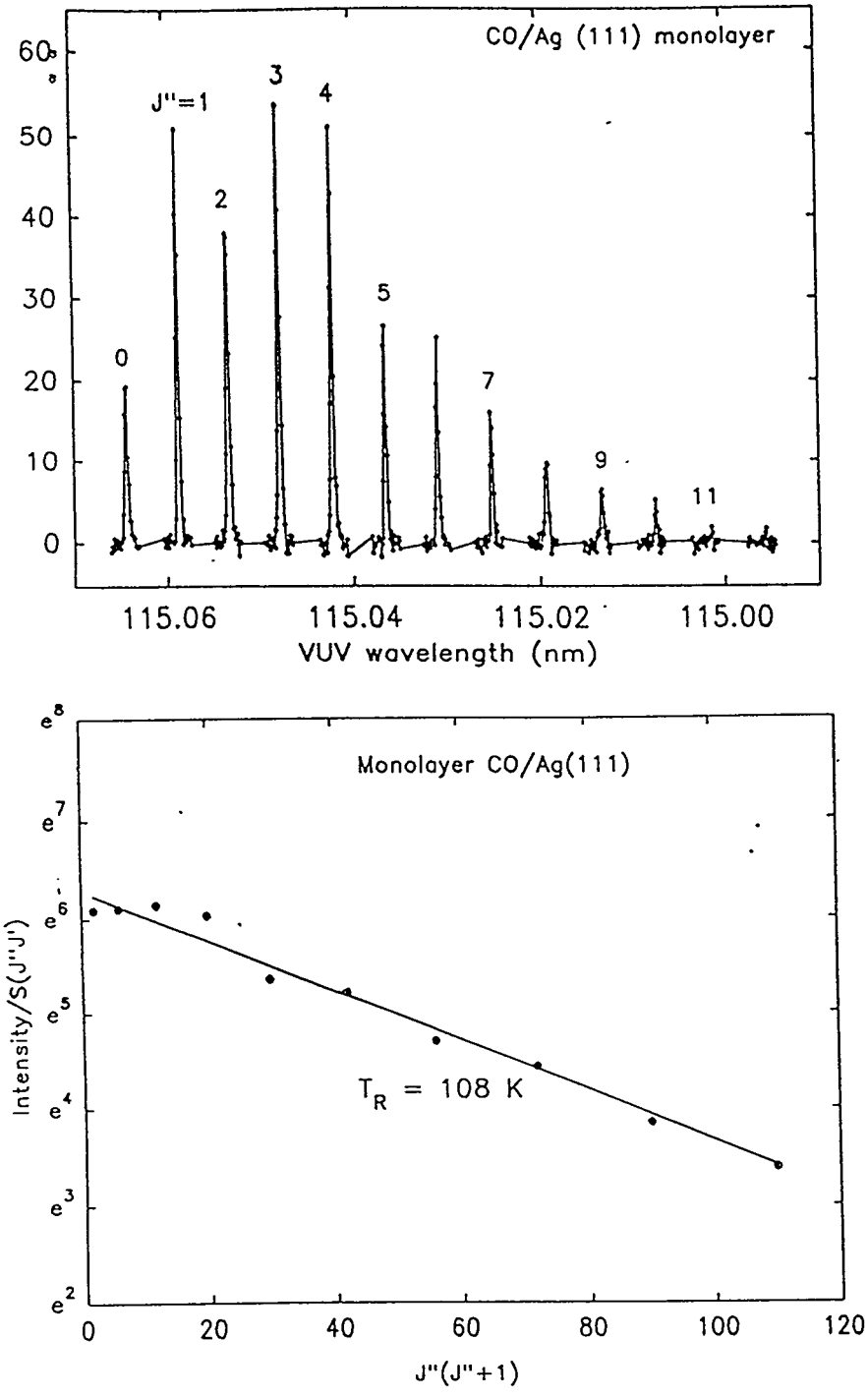

Figure 5: Upper panel: Resonant (VUV+UV) multiphoton ionization spectrum of CO via the $B-X$ transition following IR-desorption from Ag(111). The spectrum was taken for CO molecules desorbed with a velocity of 350 m/sec. Lower panel: Boltzmann plot of the rotational state populations obtained by the REMPI spectrum. The straight line represents a least squares fit from which a rotational temperature of 108 K is derived.

light at 1064 nm and incident at 45° is $R \sim 98\%$.[15] These quantities result in a calculated ΔT_{max} of $2-4$ K which, according to the observed TDS curves (see Fig. 2), is smaller than that required to induce thermal desorption from the monolayer (48 K) or multilayer (36 K). Clearly, these calculated transient temperatures are inconsistent with the observed desorption yields and the derived rotational and translational temperatures ($\sim$ 110 K). Given that the heat-diffusion model has been tested with considerable success,[4,5] it is likely that the small values of ΔT_{max} result from inaccurate parameter values such as the thermal constants (K and κ) and reflectivity (R) for Ag at low temperature. Specifically, the thermal constants are rapidly increasing below 50 K with the thermal diffusivity (κ) changing by an order of magnitude between 20-50 K.[25] The reflectivity is very sensitive to surface preparation and specific measurements for Ag(111) at low temperature are unavailable. Intensity inhomogeneities in the IR laser beam could also give rise to small "hot" spots which could lead to higher incident power densities (I_0) and consequently higher calculated transient temperatures. Measurements are currently underway to examine the spatial distribution of the IR beam. As an alternative to direct comparison with calculated transient temperatures, the proposed thermal desorption mechanism could be verified through power dependent measurements of the CO energy distributions which, according to the heat-diffusion model, should be proportional to I_0 (see above).

ACKNOWLEDGEMENTS

This work was performed at Brookhaven National Laboratory and supported by the US Department of Energy, Office of Basic Energy Sciences under contract No. DE-AC02-76CH00016.

References

[1] D. S. King and R. R. Cavanagh, *Advances in Chemical Physics*, K. P. Lawley, editor (John Wiley and Sons, New York, 1989), p. 45 and references therein.

[2] R. R. Cavanagh, D. S. King, J. C. Stephenson and T. F. Heinz, *J. Phys. Chem.*, **97**, 786 (1993) and references therein.

[3] J. F. Ready, *Effects of High-Power Laser Radiation*, (Academic, New York, 1971).

[4] D. Burgess, Jr., P. C. Stair and E. Weitz, *J. Vac. Sci. Technol. A*, **4**, 1362 (1986).

[5] J. M. Hicks, L. E. Urbach, E. W. Plummer and H.-L. Dai, *Phys. Rev. Lett.*, **61**, 2588 (1988).

[6] S. A. Buntin, L. J. Richter, D. S. King and R. R. Cavanagh, *J. Chem. Phys.*, **91**, 6429 (1989); S. A. Buntin, L. J. Richter, R. R. Cavanagh and D. S. King, *Phys. Rev. Lett.*, **61**, 1321 (1988); L. J. Richter, S. A. Buntin, R. R. Cavanagh and D. S. King, *J. Chem. Phys.*, **89**, 5344 (1988).

[7] J. A. Prybyla, T. F. Heinz, J. A. Meisewich and M. M. T. Loy, *Surf. Sci.*, **230**, L173 (1990).

[8] C. W. Muhlhausen, L. R. Williams, and J. C. Tully, *J. Chem. Phys.*, **83**, 2594 (1985).

[9] K. Fukutani, M.B. Song and Y. Murata, *J. Chem. Phys.*, **103**, 2221 (1995).

[10] M. Asscher, F.M. Zimmermann, L. L. Springsteen and P. L. Houston, *J. Chem. Phys.*, **96**, 4808 (1992).

[11] K. Al-Shamery, I. Beauport, H.-J. Freund and H. Zacharias, *Chem. Phys. Lett.*, **222**, 107 (1994).

[12] B. P. Stoicheff, J. R. Banic, P. Herman, W. Jamroz, P. E. LaRocque and R. H. Lipson, *Laser Techniques for Extreme Ultraviolet Spectroscopy*, T. J. McIlrath and R.R. Freeman, editors (American Institute of Physics, New York, 1982), p.19.

[13] R. G. Tonkyn and M. G. White, *Rev. Sci. Instrum.*, 60, 1245 (1989).

[14] R. T. Wiedmann and M. G. White, *High Resolution Spectroscopy with Photoelectrons*, I. Powis, editor (John Wiley and Sons, 1995), p.

[15] J. H. Weaver, C. Krafka, D. W. Lynch and E. E. Koch, *Optical Properties of Metals*, H. Behrens and G. Ebel, editors (Fachinformationszentrum, Karlsruhe, 1981)

[16] H. Rottke and H. Zacharias, *Opt. Commun.*, 55, 87 (1985).

[17] W. Hansen, M. Bertolo and K. Jacobi, *Surf. Sci.*, 253, 1 (1991).

[18] D. Schmeisser, F. Greuter, E. W. Plummer and H.-J. Freund, *Phys. Rev. Lett.*, **54**, 2095 (1985).

[19] M. F. Toney and S. C. Fain, *Phys. Rev. B*, 36, 1248 (1987); H. You and S. C. Fain, *Surf. Sci.*, **151**, 361 (1985) and references therein.

[20] J. Yoshinobu, T. H. Ballinger, Z. Xu, H. J. Jänsch, M. I. Zaki, J. Xu and J. T. Yates, Jr., *Surf. Sci.*, 255, 295 (1991)

[21] G. E. Moore, *J. Appl. Phys*, **32**, 1241 (1961); T. E. Madey and J. T. Yates, Jr., *J. Vac. Sci. Technol.*, 8, 525 (1971).

[22] G. McElhiney, H. Papp and J. Pritchard, *Surf. Sci.*, 54, 617 (1976).

[23] G. Herzberg, *Molecular Spectra and Molecular Structure: I. Spectra of Diatomic Molecules* (Van Nostrand, New York, 1950), p. 208.

[24] T. H. Hanisco, C. Yan and A. C. Kummel, *J. Chem. Phys.*, 97, 1484 (1992).

[25] C. Y. Ho, R. W. Powell and P. E. Liley, *J. Phys. Chem. Ref. Data*, 1, 279 (1972); C. Y. Ho, R. W. Howell and K. Y. Wu, *Proceedings on the 8th Conference on Thermal Conductivity*, C. Y. Ho and R. E. Tayler, editors (Plenum Press, New York, 1969), 971.

DISCLAIMER